JOURNAL OF GEOPHYSICAL RESEARCH, VOL. 94, NO. C12, PAGES 18,023–18,030, DECEMBER 15, 1989

Shear Instabilities of the Mean Longshore Current
1. Theory

A. J. BOWEN

Department of Oceanography, Dalhousie University, Halifax, Nova Scotia, Canada

R. A. HOLMAN

College of Oceanography, Oregon State University, Corvallis

A new class of nearshore waves based on the shear instability of a steady longshore current is discussed. The dynamics depend on the conservation of potential vorticity but with the background vorticity field, traditionally the role of Coriolis in larger scale flows, supplied by the shear structure of the longshore current. The resulting vorticity waves are longshore-progressive with celerities roughly equal to $V_0/3$, where V_0 is the peak longshore current velocity. A natural frequency scaling for the problem is f_s, the shear of the seaward face of the longshore current. While the instability can span a range of frequencies and wavenumbers, a representative frequency is given by $0.07 f_s$, typically in the range of 10^{-3}–10^{-2} Hz (called the Far Infragravity, or FIG, band because frequencies are just below those of the infragravity band). Wavelengths are of the order of $2x_0$, where x_0 is the width of the longshore current. Growth is exponential with an e-folding time that is typically half of a wave period. Field data, presented in the companion paper [Oltman-Shay et al., this issue], demonstrate the presence of energetic motions from a natural beach whose behavior matches the theory in many aspects. Results from the model suggest that shear instability will be more important on barred, rather than monotonic beach profiles, a result of the stronger shears expected over the bar crest. Since vorticity waves will probably have a profound effect on cross-shore mixing as well as longshore current dissipation, we expect the dynamics of barred and monotonic beaches to show fundamental differences.

Introduction

Dominant energy sources in the nearshore have long been considered to be gravity waves and mean currents or circulation. Frequency bands of gravity waves included the obvious wind wave and swell frequencies ($O(10^{-1})$ Hz) and the more recently studied infragravity frequencies ($O(10^{-2})$ Hz). The band between infragravity and mean flows has received little study, and dynamics have generally been associated with shelf-scale or atmospheric events [*Munk et al.*, 1964].

Free gravity wave motions in the infragravity band may be either leaky modes with longshore wavenumber, k, less than σ^2/g (where $\sigma = 2\pi/T$ is the frequency and g is gravitational acceleration), or trapped edge waves with larger wavenumber, $\sigma^2/g \leq k \leq \sigma^2/g\beta$, where β is the beach slope. No gravity wave motions exist for wavenumbers larger (shorter wavelengths) than this upper limit.

In the companion paper [*Oltman-Shay et al.*, 1989] (hereinafter OSHB89), field measurements of nearshore wave motions are described wherein wavelengths are an order of magnitude too short to be gravity waves. These motions occur at frequencies typically in the range (10^{-3}–10^{-2}) Hz, exceeding the traditional low-frequency limit of the infragravity band. This band has been named the Far Infragravity (FIG) band in analogy to the relationship of infrared and far infrared in the electromagnetic spectrum.

OSHB89 show the FIG band waves to be energetic and very coherent in the longshore direction. Kinematics are linked to the strength of the mean longshore current. In this paper, we present a model for these waves based on a shear instability of the mean longshore current. While new to nearshore, the mechanism is well studied in larger-scale physical oceanography (*Niiler and Mysak* [1971] for example) and depends on the conservation of potential vorticity. For the larger scale case, a background potential vorticity is supplied by the Earth's rotation through a term f/h, where f is Coriolis and h is the depth. For the nearshore Coriolis is neglected and the background vorticity is derived from the shear structure of a steady longshore current. Perturbation of the current will then lead to a longshore-progressive vorticity (or shear) wave, where the restoring force may be considered to be potential vorticity instead of the traditional gravitational acceleration. Wavelengths are substantially shorter than gravity waves of the same frequency.

In the next section we develop the basic equations for the conservation of potential vorticity for the case of a small perturbation to a steady longshore current. The equations are then solved for a simple example geometry. Under some conditions the solution is unstable so that the wave will grow exponentially. The characteristic scales of these motions are discussed and are shown to be roughly the same as the field observations of OSHB89. Finally, the impact of this new class of motions to nearshore dynamics is discussed.

Theory

Since the waves observed by OSHB89 are too short to satisfy gravity wave dynamics, we seek alternate solutions to the equations of motion. In particular, we will search for short scale motions under the nondivergent, or rigid lid, assumption. In this case, accelerations of the flow will be driven by the inertial terms involving the mean longshore current. The development follows closely that of *Niiler and Mysak* [1971] for the case of continental shelf waves.

The shallow water, inviscid equations for horizontal momentum are

$$u_t' + \mathbf{u}' \cdot \nabla u' = -g\eta_x$$
$$v_t' + \mathbf{u}' \cdot \nabla v' = -g\eta_y \qquad (1)$$

where x and y are the horizontal coordinates (x being positive

Paper number 89JC01393.
0148-0227/89/89JC-01393$05.00

offshore from the shoreline) with corresponding velocity components $\mathbf{u}' = (u', v')$, η is the sea surface elevation, t is time, g is gravitational acceleration and ∇ is the horizontal gradient operator. Subscripts indicate partial differentiation. Coriolis force is neglected since a typical frequency, σ, is much greater than Coriolis ($\sigma/f \approx 10^2$).

We assume that the total flow consists of a steady longshore current, $V(x)$, and a small perturbation, $\mathbf{u}$, such that $\mathbf{u}' = [u(x, y), v(x, y)+V(x)]$ and $u, v \ll V$. Substituting and retaining only the terms that are linear in the perturbation velocity, we have

$$u_t + Vu_y = -g\eta_x$$
$$v_t + uV_x + Vv_y = -g\eta_y \tag{2}$$

Under the assumption of nondivergence, η_t is assumed negligible in comparison to horizontal fluxes, so that the conservation of mass equation becomes

$$\nabla \cdot (h\mathbf{u}') = (hu)_x + (hv)_y = 0 \tag{3}$$

where the bottom is at $z = -h(x)$, assuming a two-dimensional beach profile. From (3), we may represent $\mathbf{u}$ in terms of a stream function, Ψ, such that $\nabla \times \Psi = (h\mathbf{u})$, or

$$(hu) = -\Psi_y$$
$$(hv) = \Psi_x \tag{4}$$

Cross-differentiating (2) to remove η, and substituting the stream function yields

$$\left(\frac{\partial}{\partial t} + V\frac{\partial}{\partial y}\right)\left(\frac{\Psi_{yy}}{h} + \left(\frac{\Psi_x}{h}\right)_x\right) = \Psi_y\left(\frac{V_x}{h}\right)_x \tag{5}$$

which is just the linearized version of the equation for the conservation of potential vorticity,

$$\frac{D}{Dt}\pi_s = \left(\frac{\partial}{\partial t} + \mathbf{u}' \cdot \nabla\right)\left(\frac{\zeta + V_x}{h}\right) = 0 \tag{6}$$

We define $\pi_s \equiv (\zeta+V_x)/h$ as the potential vorticity of the flow, consisting of a relative vorticity, $\zeta/h = (v_x-u_y)/h$, and a "background" vorticity, V_x/h, arising from the shear of the longshore current. Equation (6) just expresses the conservation of potential vorticity, in analogy to the conservation of potential vorticity in larger scale geophysical flows, but with the shear, V_x, taking the role of Coriolis, f. More specifically, equation (5) states that changes in the relative vorticity (left-hand side) will be caused by cross-shore perturbations (Ψ_y) of the background vorticity (right-hand side). This vorticity response acts as a restoring force for the perturbation.

We assume a solution of the form

$$\Psi = \Re\mathbf{e}\left\{\psi(x)\, e^{i(ky-\sigma t)}\right\} \tag{7}$$

where we assume the longshore wavenumber, k, is real, but σ and ψ may be complex. $\Re\mathbf{e}$ indicates the real component. Substituting (7) in (5) yields an eigensystem in $c_p = \sigma/k$ and ψ,

$$(V - c_p)\left(\psi_{xx} - k^2\psi - \frac{\psi_x h_x}{h}\right) - h\psi\left(\frac{V_x}{h}\right)_x = 0 \tag{8}$$

Solutions will be vorticity waves or shear waves with phase velocity c_p and cross-shore structure $\psi(x)$. Of particular interest is the case when the eigenvalue is complex, such that σ has a positive imaginary component, $\sigma = \sigma_{re}+i\,\sigma_{im}$. The result is an instability in the form of a progressive wave with an exponentially growing amplitude

$$\Psi = \exp(\sigma_{im} t)\,\Re\mathbf{e}\left\{\psi(x)\exp[i(ky - \sigma_{re} t)]\right\} \tag{9}$$

It can be shown that a necessary condition for this instability is the existence of an extremum of the background potential vorticity, V_x/h, in the interval $0 < x < \infty$ (*Rayleigh* [1880] with minor extension).

Vorticity Waves for a Simple Topography

The essential dynamics of shear waves can be illustrated with an extremely simple example. Consider the case of a flat-bottom beach of depth h_0 bordered by a coastal wall at $x = 0$ (Figure 1). The longshore current has width x_0 with a maximum current, V_0, at location $x = \delta x_0$. This divides the x plane into a region of positive linear shear (region I), a region of negative linear shear (region II), and a region extending to $x = \infty$ of zero longshore current (region III). Superimposed on Figure 1 is the distribution of background potential vorticity, V_x/h. The existence of an extremum in region II suggests the possibility of unstable (growing) wave solutions.

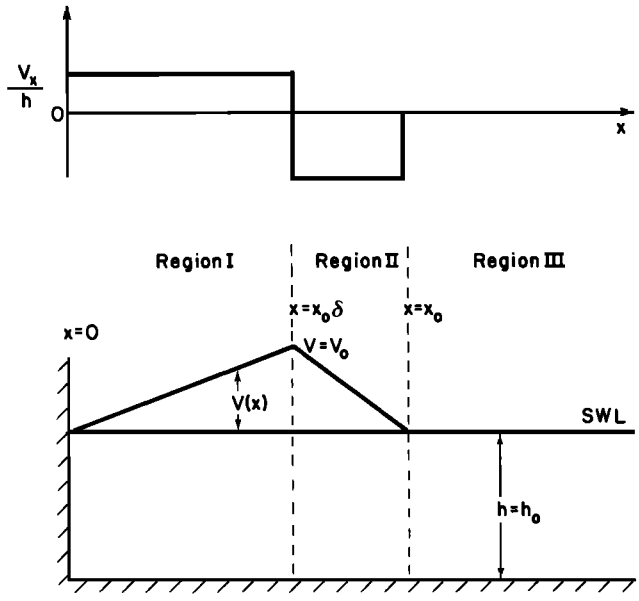

Fig. 1. Longshore current geometry and bathymetry showing the three regions of the example calculations. Upper panel shows the background potential vorticity distribution.

In each of the three regions, (8) reduces to

$$\psi_{xx} - k^2\psi = 0 \tag{10}$$

which has solutions

$$\begin{aligned} &\text{Region I} && \psi_I = A_1 \sinh(kx) \\ &\text{Region II} && \psi_{II} = A_2 \sinh(kx) + B_2 \cosh(kx) \\ &\text{Region III} && \psi_{III} = A_3 e^{-kx} \end{aligned} \tag{11}$$

where we have taken the shoreline and far-field boundary conditions to be $\psi(0) = \psi(\infty) = 0$ (no flow through the beach and no mean longshore flow associated with the perturbation). For interior boundary conditions we require ψ and pressure (or sea surface elevation) to be continuous. From (2), the latter condition implies that

$$\eta = -\frac{1}{gh}\left[(V - c_p)\,\psi_x - V_x\psi\right] \tag{12}$$

must be continuous. Applying the boundary conditions at $x = \delta x_0$, we have

$$\frac{B_2}{A_2} = \frac{S_\delta^2 \Delta V_x}{(V_0 - c_p)\,k - C_\delta S_\delta\,\Delta V_x} \tag{13}$$

We have used the short forms $S_\delta = \sinh(kx_0\delta)$, $C_\delta = \cosh(kx_0\delta)$, and $\Delta V_x = (V_{x_1} - V_{x_2})$, the difference between the linear shears in the two regions. Similarly, at $x = x_0$, we have

$$\frac{B_2}{A_2} = -\frac{\sigma + V_{x_2} S_0 E_0}{\sigma + V_{x_2} C_0 E_0} \tag{14}$$

where $S_0 = \sinh(kx_0)$, $C_0 = \cosh(kx_0)$, and $E_0 = \exp(-kx_0)$. Equating (13) and (14) yields, after considerable simplification, a quadratic expression for σ

$$a\sigma^2 + b\sigma + c = 0 \tag{15}$$

where

$$a = 1$$

$$b = -kV_0\left[1 - \frac{(1 - e^{-2kx_0\delta})}{2kx_0\delta(1-\delta)} + \frac{(1 - e^{-2kx_0})}{2kx_0(1-\delta)}\right] = -kV_0 F(kx_0, \delta)$$

$$c = k^2V_0^2\left[\frac{(1 - e^{-2kx_0})}{2kx_0(1-\delta)} - \frac{(1 - e^{-2kx_0\delta})(1 - e^{-2kx_0(1-\delta)})}{(2kx_0)^2(1-\delta)^2\delta}\right] \tag{16}$$

Time and Length Scales

For any k, equation (15) will have two roots which may either be both real or complex conjugates depending on the sign of $(b^2 - 4ac)$. The latter case, yielding exponentially growing waves (equation 9), is the case of interest.

An example result is shown in Figure 2 for longshore current geometry $(V_0, \delta, x_0) = (1.0\ \text{ms}^{-1}, 0.5, 100\ \text{m})$, reasonable values for comparison with Figure 6 of OSHB89. For k less than a lower limit or higher than an upper limit, there exist two real roots. These are shear waves that are stable but which would rapidly decay in the presence of dissipation. For wavelengths, $L = 2\pi/k$, in an intermediate range (190 m < L < 435 m for this geometry) σ is complex and the waves grow exponentially. Through this region of instability, the phase velocity of the vorticity waves will be given by

$$c_p = \frac{\Re e(\sigma)}{k} = -\frac{b}{2k} = \frac{V_0}{2} F(kx_0, \delta) \tag{17}$$

Thus for a particular geometry of the longshore current, c_p varies linearly with the strength of the longshore current, V_0. Figure 3*a* shows that $F(kx_0, \delta)$ is always positive and is only a weak function of L/x_0 (= $2\pi/kx_0$) and δ through the unstable range of wavenumber. Thus vorticity waves on this geometry will always propagate in the direction of the mean current with a speed of 1/4 to 1/2 the peak longshore current velocity.

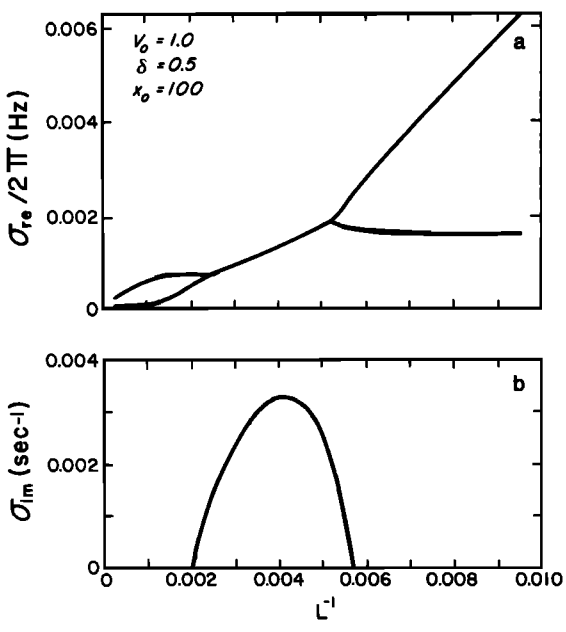

Fig. 2. Frequency-wavenumber plots of the shear instability for the example geometry: Figure (*a*) real and (*b*) imaginary components. Wave motions for which $\sigma_{im} > 0$ are unstable and will grow exponentially at a rate proportional to σ_{im}. The motion for which σ_{im} is a maximum is used to determine characteristic scales of the waves.

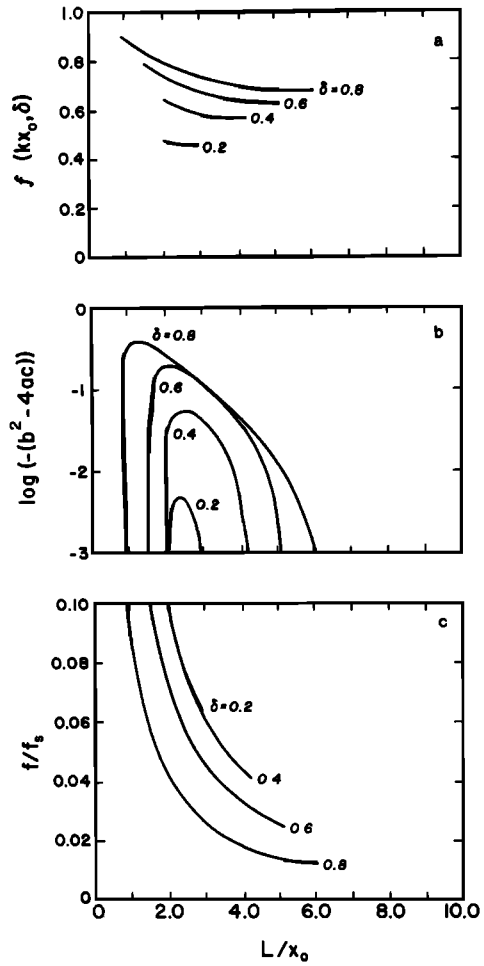

Fig. 3. (*a*) The shape factor $F(kx_0, \delta)$ from the b term in equation (15). (*b*) The quantity $-(b^2-4ac)$ from which the magnitude of the imaginary frequency is calculated. Only the unstable region is shown. (*c*) Frequencies of the instability normalized by the offshore shear, f_s.

The existence and strength of the instability depend on the sign and magnitude of the quantity (b^2-4ac). Figure 3*b*, a plot of the quantity $-(b^2-4ac)$ versus L/x_0 for the instability regime, shows that the wavenumber range of the instability depends on δ, with the mechanism being narrow-banded for small δ but quite broad for large δ. Figure 3*c* shows the corresponding wave frequencies, f (= $1/T$), normalized by f_s, the shear on the seaward side of the longshore current,

$$f_s = \frac{V_0}{x_0(1-\delta)} \tag{18}$$

The instability exists from a high-frequency limit of approximately 0.1 f_s to a low frequency limit that varies with δ. If scientific interest is focussed on conditions of large δ and large shear f_s (yielding the fastest growth rates), then the span of frequencies can be quite large.

While the instability occurs over a range in frequency and wavenumber, there will be a single fastest growing wave that we can use to determine characteristic time and length scales. This corresponds to the point of maximum σ_{im} (Figure 2*b*). Figure 4*a* shows the frequency, f_f, of the fastest growing vorticity wave, normalized by f_s. Figure 4*b* shows the maximum growth rate, f_g, also normalized by f_s, while Figure 4*c* shows the corresponding wavelength normalized by x_0, the width of the entire longshore current.

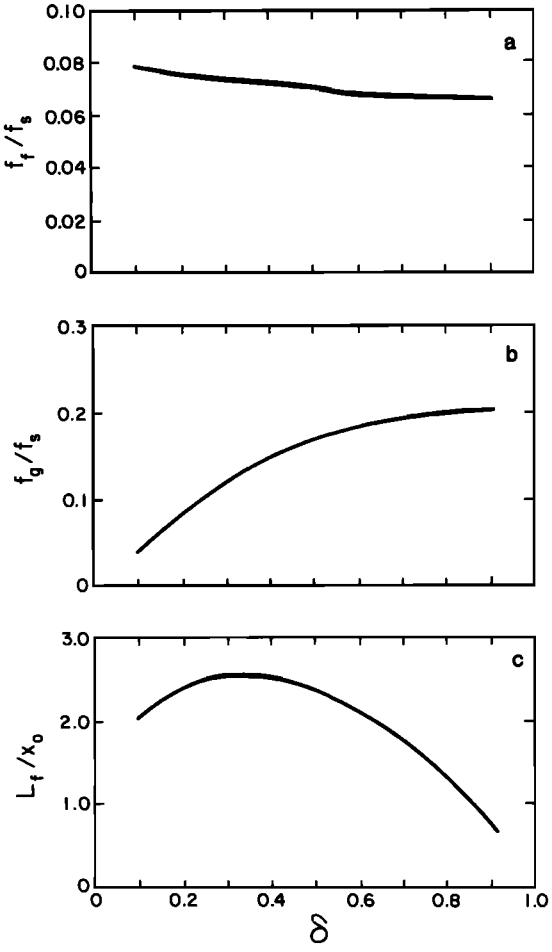

Fig. 4. (*a*) Characteristic frequencies, f_f, (*b*) growth rates, f_g, and (*c*) wavelengths, L_f, of the fastest growing wave as a function of the longshore current geometry.

For the geometry under consideration, it is apparent that f_s and x_0 provide appropriate temporal and spatial scaling, respectively. As normalized, the variables depend only on δ, and even then, the dependence is weak (particularly for the wave frequency, f_f). From Figure 4, rough scales for the fastest growing instabilities will be

$$f_f \approx 0.07\, f_s$$
$$\sigma_{im} \approx (0.1 - 0.2)\, f_s \approx (1 - 3)\, f_f \qquad (19)$$
$$L_f \approx (1 - 3)\, x_0$$

For the example longshore current geometry of Figure 2, we find $T_f = 1/f_f = 753$ s and $L_f = 250$ m, clearly in the range of the low-celerity motions observed in OSHB89, and substantially shorter than the $O(10$ km $)$ wavelength of the shortest gravity wave (mode 0 edge wave) of this frequency. The growth time scale ($= \sigma_{im}^{-1}$) gives a characteristic, *e*-folding time scale for the instability of 300 s, substantially faster than one period. Clearly, this is a strong instability and the assumption of linearity in the perturbation would not be valid for long.

Spatial Structure of Shear Waves

Knowing σ, we may now calculate the spatial structure of the wave motions. The coefficients are found from the interior boundary conditions, where

$$A_1 S_\delta = A_2 S_\delta + B_2 C_\delta$$
$$A_3 S_0 = A_2 S_0 + B_2 C_0 \qquad (20)$$
$$\frac{B_2}{A_2} = -\frac{\sigma + V_{x_2} S_0 E_0}{\sigma + V_{x_2} C_0 E_0}$$

If we chose $A_2 = a$, then we see from (20) that for frequencies in the unstable range (σ complex), B_2 will be complex. In this case A_1 and A_3 will also be complex. Since fluid motions are associated only with the real component of ψ, we can incorporate the complex coefficients into a phase shift, θ, such that

Regions I and III

$$\theta = \tan^{-1}\left(\frac{A_{im}}{A_{re}}\right) \qquad (21)$$

Region II

$$\theta = \tan^{-1}\left(\frac{B_{im}\cosh(kx)}{a\sinh(kx) + B_{re}\cosh(kx)}\right)$$

That is, the phases in region I and in region III will be constant but not necessarily the same. In region II, the phase will vary with cross-shore position. Figure 5*a* shows the real and imaginary

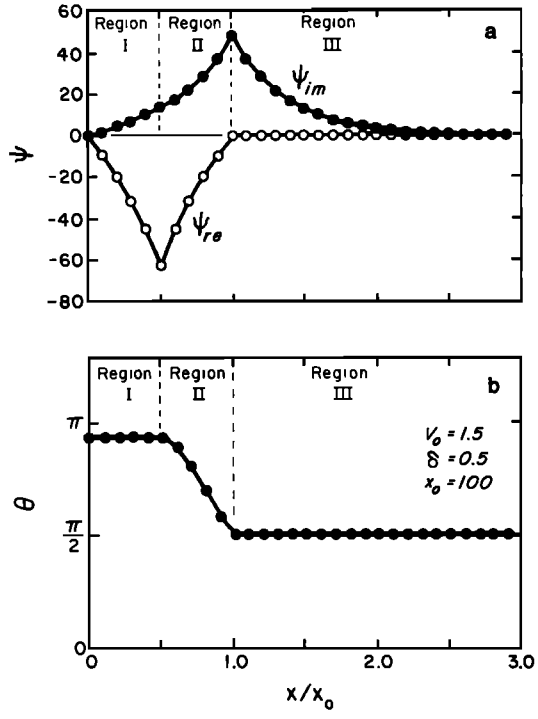

Fig. 5. (*a*) Real and imaginary components of the stream function, ψ, as a function of cross-shore distance. (*b*) Cross-shore phase shift of the stream function.

components of $\psi(x)$ and Figure 5*b* shows the phase, $\theta(x)$, for the fastest growing instability for the longshore current geometry (V_0, δ, x_0) = (1.5 ms^{-1}, 0.5, 100 m). These plots confirm the rather complicated nature of the motions in region II. Moreover, it can be seen that ψ_x (hence v) is not continuous. This non-physical behavior stems from the non-physical discontinuities in V_x in the original geometry. In contrast, cross-shore velocities will be continuous. The surface elevation signal of the vorticity waves may be found by equation (12). Magnitudes tend to be much smaller than for gravity waves, scaling roughly as $V_0/2g\,|u, v| = O(5\text{cm})$.

Measurements of the local phase relationships between fluid variables are often used to distinguish classes of wave motions (standing versus progressive motions, for instance). Figure 6 shows the local phase difference between u and v (Figure 6*a*) and between u and η (Figure 6*b*) for this geometry. Interestingly, u

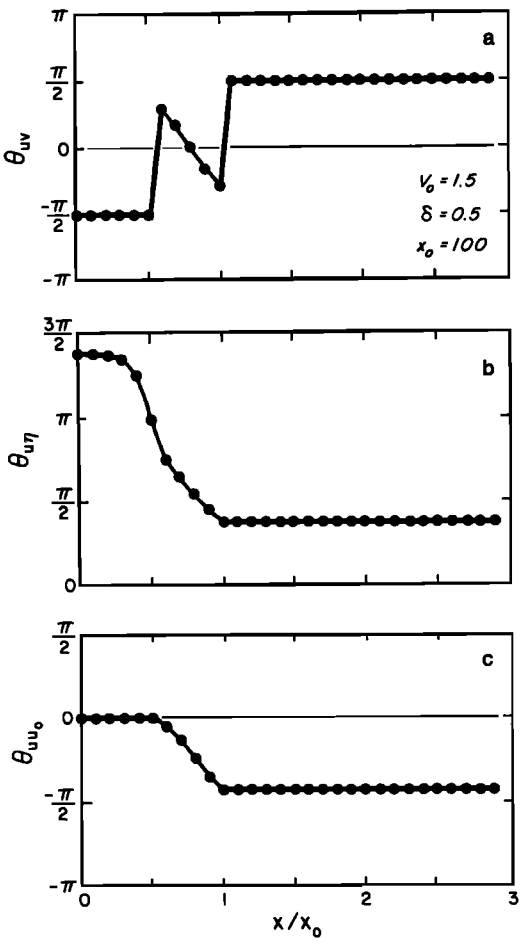

Fig. 6. Relative phase between (*a*) cross-shore and longshore velocity components, and (*b*) cross-shore velocity and sea surface elevation as a function of cross-shore position, with (*c*) showing the phase differences in the cross-shore velocity signal between the shoreline and points offshore.

and v are in quadrature in both regions I and III, although phase difference changes from a lag (u lags v by $\pi/2$) in region I to a lead in region III. The phase relationship in region II is spatially complex: u and η show phases that are relatively constant in regions I and III (although not multiples of $\pi/2$) with a transition in region II. Figure 6*c* shows the relative phase changes in cross-shore velocity, u, between the shoreline and different cross-shore locations. Again, a phase shift occurs in region II, the offshore shear region of the longshore current. It is conceivable that phase relationships measured from field data may be useful in mapping the shear structure of naturally-occurring longshore currents.

Figure 7 shows the spatial form of $\psi(x, y)$ of the fastest growing wave for this particular geometry and with depth, $h_0 = 1$ m. The pattern consists of a series of highs and lows with each offset over region II by the complex phase shift. Circulation of the vorticity wave will be along streamlines, going clockwise around highs with a velocity proportional to the local gradient. The entire pattern is progressive in the longshore direction. Figure 8 shows the spatial pattern of the total velocity, $\mathbf{u}' = V+\mathbf{u}$. The selected magnitude of the perturbation vorticity wave is arbitrary; the equations only show that the motion is unstable. For this figure, the wave motion was scaled such that $|v(x_0\delta)| = V_0$, a magnitude rather larger than our small amplitude assumption, but useful for illustration. The obvious feature is a meandering of the longshore current about its position of maximum strength. Small re-circulation cells are seen in the nearshore and offshore regions. Again, this pattern is progressive in the direction of the mean longshore current, so that a fixed current meter would see strong fluctuations over the perturbation period.

Finally, the validity of the original rigid lid assumption can be examined. The ratio of the vertical acceleration and the advective terms in the full continuity equation scales as $(V-c_{re})^2/gh \approx O(0.5^2/10) = O(0.025)$. Thus the rigid lid approximation is valid for these motions.

Discussion

The previous results demonstrate the mechanism of shear instability of a mean longshore current in the nearshore. The generated waves have phase velocities, length and time scales that are similar to those observed [OSHB89], lending support to the model. Yet the example geometry of a flat bottom beach and linear shears could be considered only a gross approximation of the natural situation. As discussed earlier, the source of the instability lies in the structure of the background potential vorticity, V_x/h (equations (6) and (8)). Figures 9*a* and 9*b* show an actual bathymetry from SUPERDUCK (the field experiment at which the OSHB89 data were collected) and a more realistic form for the longshore current, given analytically by

$$V(x) = V' x \exp[-(\alpha x)^n] \qquad (22)$$

which has a peak velocity, $V_0 = V'/(\alpha(n e)^{1/n})$ at location $x_\delta = 1/(\alpha n^{1/n})$. Reasonable values of V_0, x_δ, and n were 1.2 ms^{-1}, 90 m, and 3, respectively. Figure 9*c* shows the potential vorticity profile for this more realistic case. While the profile is smoother than that of the example, the basic structure is the same. Potential vorticity still goes from positive near the shore, through a negative minimum, then to zero offshore. The necessary condition for an instability, the existence of an extremum, is still satisfied, and we would expect the instability to scale roughly as the example. In general, it will be true that the structure of potential vorticity will be based more on the velocity structure than on the beach profile; the velocity shear can change sign, whereas depth is always positive.

The shear of the seaward face of the current, f_s, appears to provide a natural scaling for the frequencies of the instability. We expect the greatest scientific interest to focus on conditions of large offshore shear since growth rates will be fastest (strongest instability) and wave frequencies will be largest and most easily resolved. This suggests that the shear wave instability mechanism may be more important on barred beaches (where the concentration of wave breaking on the bar crest should force a large shear) than on monotonic profiles.

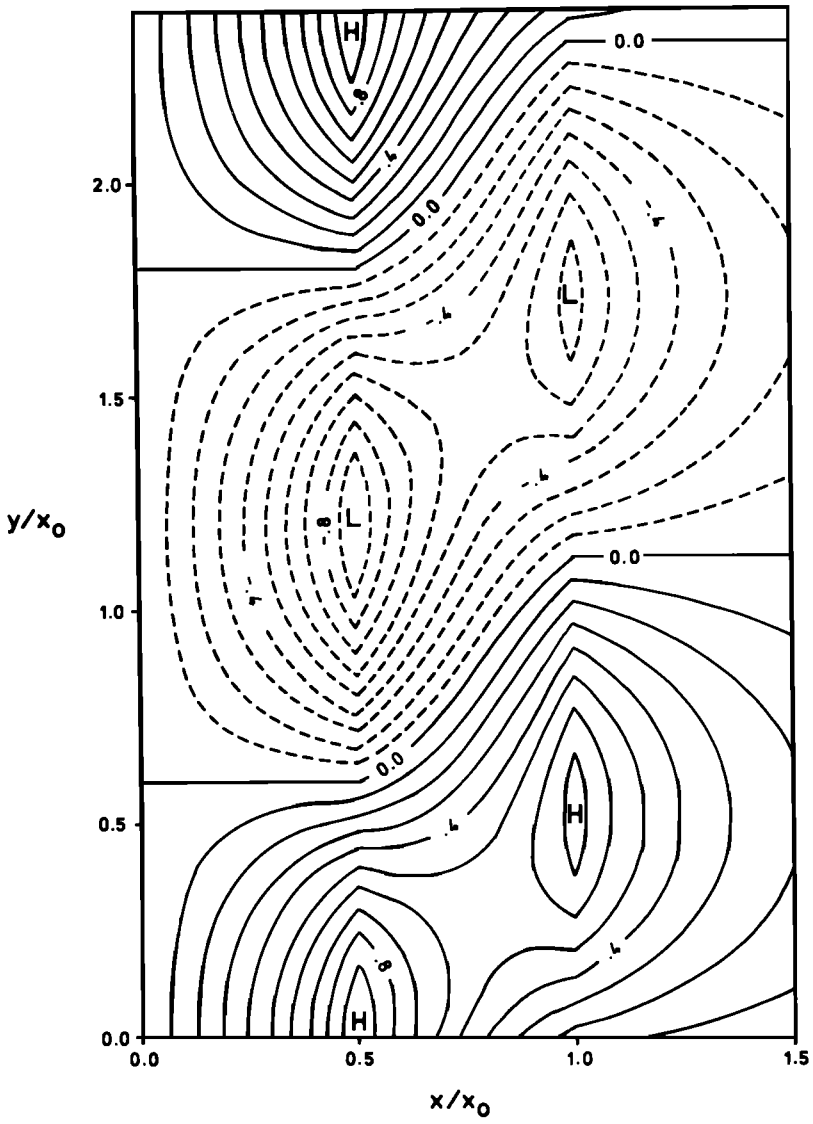

Fig. 7. Stream function pattern for one wavelength of a shear wave. The motion decays exponentially offshore. The pattern is progressive in the positive y direction.

The present model is inviscid, showing only the growth of an instability. The proper inclusion of viscosity may be difficult since advective terms will also be required. As a rough approximation we can investigate the consequences of including a linearized friction of the form $-\lambda\mathbf{u}$. In this case, dissipation can be incorporated into the imaginary component of frequency, σ_{im}, so that growth will occur as $\exp[(\sigma_{im}-\lambda)t]$. Thus the instability will be damped unless σ_{im} is greater than dissipation. However, once $\sigma_{im} > \lambda$, the instability will suddenly start to grow. If we take $\lambda = C_d V h^{-1}$, then typical values of λ will be $O(10^{-2}$–$10^{-3})$, so growth will not occur unless σ_{im} is greater than this value. Thus shear waves are theoretically expected to be less important on monotonic profiles where the offshore shear, f_s, is not large and σ_{im} is expected to be small.

In contrast to edge waves or leaky modes, for any frequency of shear wave there is only a single wavenumber (for a particular longshore current geometry). Thus lag coherence plots for shear wave dominated bands should be more coherent than those where a suite of edge waves and leaky modes are important. Increases of wavenumber bandwidth beyond the expected resolution of the analysis would result only from fluctuations in mean longshore current strength (over time scales longer than a shear wave period) and would have a relative magnitude $\Delta k/k \approx \Delta V/V$, where ΔV is the unsteadiness of the mean longshore current. Waves from days of stationary and homogeneous longshore current may be very coherent in the longshore.

Shear waves may have several important consequences to nearshore dynamics. Previously, dissipation of longshore currents was assumed to be simply through bottom friction. This mechanism shows that strong longshore currents can be unstable. The dissipation of the instability would undoubtedly be only poorly modelled by traditional dissipation terms. Moreover, the dissipation will depend not just on the magnitude of the current, but also on the maximum shear, a characteristic that will distinguish barred from monotonic beach profiles.

As shown in Figure 8, shear waves can also act as a strong mechanism for mixing in the cross-shore. If we parameterize horizontal mixing with a horizontal eddy diffusivity, $A_H \approx UX$, where U and X are characteristic cross-shore velocity and cross-shore displacement scales of the mixing agent, then we can

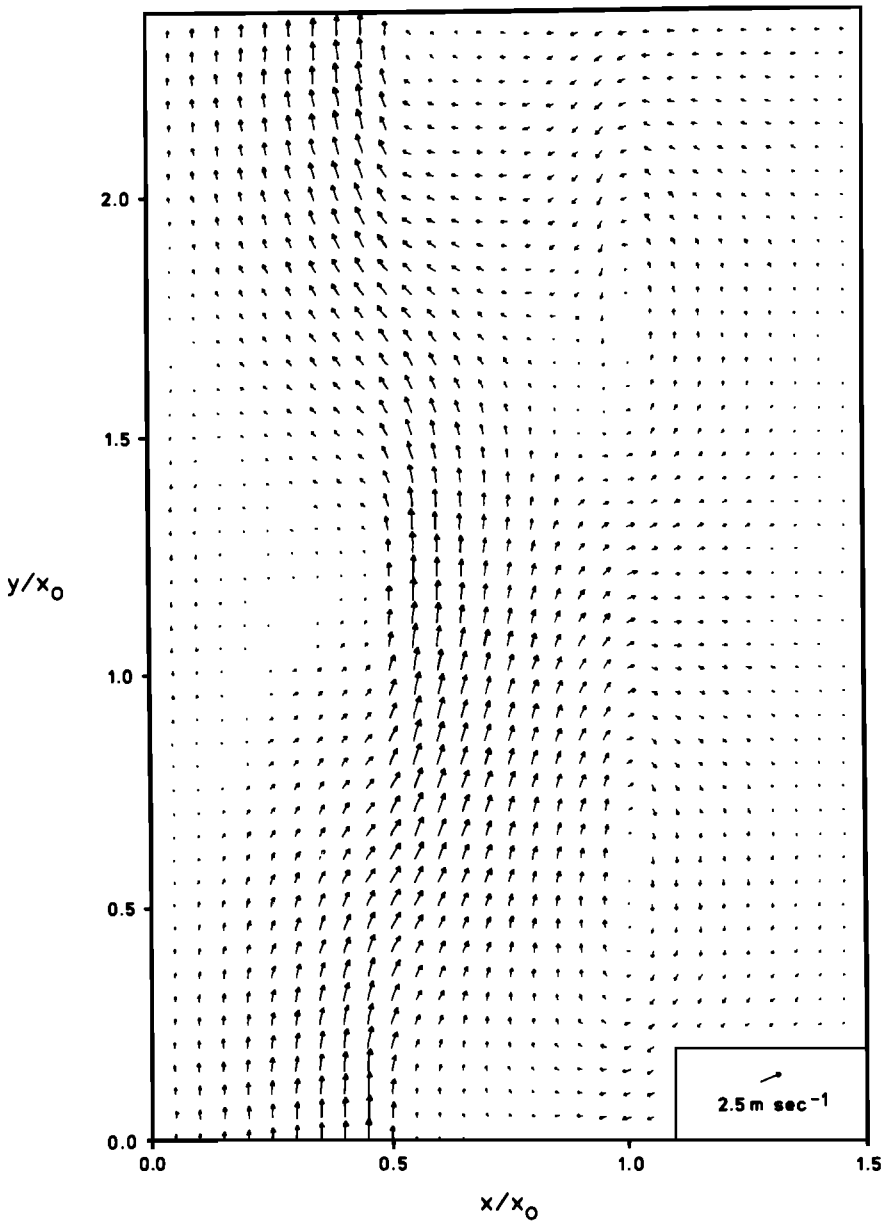

Fig. 8. Total velocity pattern for one wavelength of the wave motion. The shear wave has been scaled so that its peak magnitude equals the peak longshore current, V_0. The motion is progressive in the direction of the longshore current.

compare the relative roles of incident and shear waves in mixing. Both will have similar velocities, but an excursion scale of the shear waves may be 50 m (Figure 8), compared to approximately 5 m for incident wave. Thus shear waves may at times be the predominant mechanism for horizontal mixing.

Given the apparent strength of this instability, it may seem odd that these motions do not dominate in more circumstances, particularly in wave tank experiments where steady longshore currents are generated. Total velocity figures (similar to Figure 8) were calculated for a variety of shear wave magnitudes. Surprisingly, for shear wave magnitudes of up to 50% of the peak longshore current, the resulting pattern appeared straight and steady, indiscernible by eye from the steady flow alone. Thus wave tanks experiments may in fact be contaminated with shear wave motions that, in the limited length of the tank, have not grown to sufficient size to be detectable by rudimentary means. Contamination may become a problem for long tanks (relative to the width of the longshore current) or for a longshore currents in a spiral wave tank.

Conclusions

It has been shown that a steady longshore current in the nearshore can support oscillations that are not gravity waves, but which are much shorter scale shear waves (or vorticity waves). The underlying mechanism is the conservation of potential vorticity, the same as for larger scale oceanographic flows, but with the shear of the longshore current, V_x, playing the traditional role of Coriolis. Thus a perturbation across the background potential vorticity, V_x/h, will be balanced by a relative vorticity in the water column which acts as a restoring force.

The mechanism may be unstable if an extremum of background potential vorticity exists in the region (true for all longshore

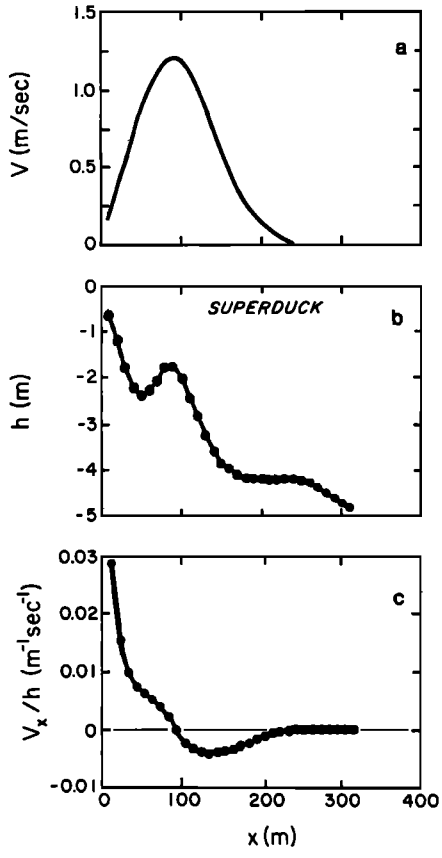

Fig. 9. (*a*) More realistic profile of longshore current. Analytical form is given by (22) with $V_0 = 1.2$ ms^{-1}, $x_\delta = 90$ m, and $n = 3$. (*b*) Representative bathymetry from the barred beach at Duck during the SUPERDUCK experiment. (*c*) Resulting potential vorticity profile.

currents on natural beaches). In that case, the perturbation may grow with an initial growth rate that is exponential. For a simple example geometry, the celerity of these motions is shown to vary as approximately 1/3 V_0, where V_0 is the peak longshore current. A natural frequency scaling of the motions is f_s, the shear on the seaward side of the longshore current. The instability occurs for a range of frequencies from about 0.1 f_s to a lower limit depending on δ, the relative location of the peak velocity in the mean longshore current. If we take the fastest growing waves as representative, the characteristic longshore wavelength is of order $2x_0$, where x_0 is the width of the longshore current. A characteristic frequency will be 0.07 f_s and growth (*e*-folding) time scale will be about half of one period. Obviously the instability is strong and assumptions of linearity would soon fail. Inclusion of a simple Rayleigh damping factor, λ, suggests that the instability will not grow unless the calculated growth rate is faster than λ, which should be $O(10^{-2}$–$10^{-3})$ Hz.

Spatial patterns of velocity depend on the relative magnitude of the shear wave and the mean current. For shear wave magnitudes less than 1/2 the peak longshore current, the vorticity wave may appear negligible to the eye (although clearly detectable to instruments). For shear waves that are comparable to V_0, the resulting pattern is one of a clearly meandering longshore current. The relative phase between wave variables u, v, and η vary with cross-shore position; these expected variations may prove useful in inferring the shear structure of naturally occurring longshore currents from measured phase relations. It is expected that the very simple geometry of the model will reproduce the important features of more realistic bathymetries and current structures since it mimics the essential elements of the potential vorticity structure.

Based on simple scaling arguments, shear waves are expected to provide an effective horizontal eddy viscosity that can be up to 10 times greater than that for incident band gravity waves. Similarly, the ultimate dissipation of longshore currents may depend critically on the shear instability, with the traditional dissipation models providing only a crude approximation of the true mechanism. These latter conclusions depend on the existence of the instability, which in turn depends on the offshore shear, f_s. Thus barred beaches, where longshore current shear can be concentrated near the bar crest, may exhibit fundamentally different dynamics than monotonic beaches.

Acknowledgments. Much of this work was carried out while R.A.H. was on sabbatical at Dalhousie University, and he would like to thank the oceanography group for their kind hospitality, stimulating environment and donuts. The entire study resulted from FIG band observations made by Joan Oltman-Shay, Peter Howd, and Bill Birkemeier during SUPERDUCK and has benefited from lively discussions with them. The authors would also like to thank Ed Thornton, Tony Dalrymple, Jurgen Battjes, and Dave Hebert for useful discussions on the impact of FIG waves. As always, we would like to thank the staff of the Field Research Facility and Curt Mason, without whose efforts none of this would have happened. Continuing and appreciated support for R.A.H. was supplied by Office of Naval Research, Coastal Sciences program, under contract N00014-87-K0009. A.J.B. is funded by National Science and Engineering Research Council, Canada.

REFERENCES

Munk, W., F. Snodgrass, and F. Gilbert, Long waves on the continental shelf: An experiment to separate leaky and trapped modes, *J. Fluid Mech.*, *20*(4), 529–544, 1964.

Niiler, P. P., and L. A. Mysak, Barotropic waves along an eastern continental shelf, *Geophys. Fluid Dyn.*, *2*, 273–288, 1971.

Oltman-Shay, J., P. A. Howd, and W. A. Birkemeier, Shear instabilities of the mean longshore current, 2, Field Observations, *J. Geophys. Res.*, this issue.

Rayleigh, Lord (J. W. Strutt), On the stability, or instability, of certain fluid motions, *Proc. London Math. Soc.*, *11*, 57–70, 1880.

A. J. Bowen, Department of Oceanography, Dalhousie University, Halifax, Nova Scotia, Canada B3H-4J1.

R. A. Holman, College of Oceanography, Oregon State University, Corvallis, OR 97331.

(Received March 1, 1989;
accepted May 6, 1989.)